

The Effects of Protonation on the Structure, Stability, and Thermochemistry of Carbon-Centered Organic Radicals

Paul M. Mayer,^{1a,b} Mikhail N. Glukhovtsev,^{1a,c} James W. Gauld,^{1a,d} and Leo Radom^{*,1a}

Contribution from the Research School of Chemistry, Australian National University, Canberra, ACT 0200, Australia

Received August 15, 1997[⊗]

Abstract: The effects of protonation on the geometries and stabilization energies of prototypical $\cdot\text{CH}_2\text{X}$ radicals (X = NH₂, OH, OCH₃, PH₂, SH, F, Cl, Br, CN, CHO, and NO₂) have been studied with the use of ab initio molecular orbital calculations at the G2 level. The proton affinities at X of the $\cdot\text{CH}_2\text{X}$ radicals and the analogous substituted methanes, CH₃X, are compared and the corresponding heats of formation calculated. For π -donor substituents (X = NH₂, OH, OCH₃, PH₂, SH, F, Cl and Br), protonation at X leads to considerable $^+\text{C}:\text{XH}$ character for both CH₃XH⁺ and $\cdot\text{CH}_2\text{XH}^+$, resulting in substantially lower heterolytic bond dissociation enthalpies and longer C–X bonds. Protonation also strengthens the C–H bonds in CH₃XH⁺ and, in combination with the reduced interaction of the lone pair on X with the singly-occupied orbital at the radical center in the radicals, results in negative radical stabilization energies for $\cdot\text{CH}_2\text{XH}^+$. For the π -acceptor substituents (CN, CHO, and NO₂), protonation enhances hyperconjugative electron donation from the methyl group to the π^* orbital of X, thereby resulting in C–X bonds in CH₃XH⁺ and $\cdot\text{CH}_2\text{XH}^+$ that are shorter than those in the unprotonated species. This also leads to weaker C–H bonds and, together with enhanced delocalization of the unpaired electron in the radical, leads to positive radical stabilization energies for $\cdot\text{CH}_2\text{XH}^+$. The proton affinities of the radicals with π -donor substituents are 30–70 kJ mol⁻¹ lower than those of their closed-shell counterparts. This may be attributed to the decreased availability of the lone-pair orbital(s) on X, resulting from interaction with the singly-occupied orbital at the radical center. The $\cdot\text{CH}_2\text{CHO}$ and $\cdot\text{CH}_2\text{NO}_2$ radicals have proton affinities that are similar to those of their closed-shell counterparts because protonation takes place in a plane almost orthogonal to the singly-occupied orbital on C, and so there is less effect in going from CH₃X to $\cdot\text{CH}_2\text{X}$.

Introduction

Protonated molecules are of interest to chemists since they are often important intermediates in reaction mechanisms. The proton affinity (PA) is a key thermochemical quantity of relevance to the chemistry of protonated molecules. It is defined as the negative of the enthalpy change in the protonation reaction:



The proton affinities (PA) of many molecules have been compiled in widely-used thermochemical compendia by Lias et al.,^{2,3} and more recent experimental studies by Mautner⁴ and McMahon⁵ have led to a number of firmly established values. Uggerud⁶ has recently reviewed the experimental techniques used to study the thermochemistry and reactivity of protonated molecules. Most recently, Hunter and Lias⁷ have produced an updated compendium of proton affinities.

The effect of protonation on molecular structure has been studied computationally by Yáñez, Mó, and co-workers.^{8–10} They found that protonation of an electronegative atom in a molecule usually leads to lengthening of the bonds to that atom. This behavior was rationalized by first noting that protonation of a substituent leads to an increase in its electronegativity. For first-row groups, the Pauling-type electronegativities are 3.98 for X = F and 5.22 for X = FH⁺; 3.44 for OH and 4.13 for OH₂⁺; and 3.04 for NH₂ and 3.58 for NH₃⁺.¹¹ Yáñez et al. argued that since protonation increases the electronegativity of X, the surrounding bonds are depopulated and therefore lengthened.^{8–10} Interestingly, Boyd et al.^{11–13} have shown computationally that the C–X homolytic bond dissociation enthalpy (BDE) is actually larger in CH₃XH⁺ than in CH₃X, a result seemingly at variance with the lengthening of the C–X bond. They explained this behavior by noting that heterolysis rather than homolysis is generally the lower energy dissociation process in the protonated species, particularly for highly electronegative X, and that the heterolytic BDEs are indeed

[⊗] Abstract published in *Advance ACS Abstracts*, December 15, 1997.

(1) (a) Australian National University. (b) Present address: Department of Chemistry, University of Ottawa, Ottawa, Canada K1N 6N5. (c) Present address: Department of Chemistry and Biochemistry, University of Delaware, Newark, DE 19716. (d) Present address: Department of Quantum Chemistry, Uppsala University, P.O. Box 518, S-751 20, Uppsala, Sweden.

(2) Lias, S. G.; Liebman, J. F.; Levin, R. D. *J. Phys. Chem. Ref. Data* **1984**, *13*, 695.

(3) Lias, S. G.; Bartmess, J. E.; Liebman, J. F.; Holmes, J. L.; Levin, R. D.; Mallard, W. G. *J. Phys. Chem. Ref. Data* **1988**, *17*, Suppl. 1.

(4) Meot-Ner (Mautner), M.; Sieck, L. W. *J. Am. Chem. Soc.* **1991**, *113*, 4448 and references therein.

(5) Szulejko, J. E.; McMahon, T. B. *J. Am. Chem. Soc.* **1993**, *115*, 7839 and references therein.

(6) Uggerud, E. *Mass Spectrom. Rev.* **1992**, *11*, 389.

(7) Hunter, E. P.; Lias, S. G. *Proton Affinity Evaluation*; in NIST Standard Reference Database Number 69; Mallard, W. G., Linstrom, P. J., Eds.; February 1997; National Institute of Standards and Technology: Gaithersburg, MD.

(8) Bordejé, M. C.; Mó, O.; Yáñez, M.; Herreros, M.; Abboud, J.-L. M. *J. Am. Chem. Soc.* **1993**, *115*, 7389.

(9) Alcamí, M.; Mó, O.; Yáñez, M.; Abboud, J.-L. M.; Elguero, J. *Chem. Phys. Lett.* **1990**, *172*, 471.

(10) Bouchoux, G.; Drancourt, D.; Leblanc, D.; Yáñez, M.; Mó, O. *New J. Chem.* **1995**, *19*, 1243.

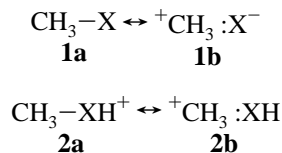
(11) Boyd, R. J.; Glover, J. N. M.; Pincock, J. A. *J. Am. Chem. Soc.* **1989**, *111*, 5152.

(12) Boyd, S. L.; Boyd, R. J.; Bessonette, P. W.; Kerdraon, D. I.; Aucoin, N. T. *J. Am. Chem. Soc.* **1995**, *117*, 8816.

(13) Boyd, S. L.; Boyd, R. J. *J. Am. Chem. Soc.* **1997**, *119*, 4214.

much lower in protonated molecules than they are in neutral molecules.^{12,13} The lengthening of the C–X bond following protonation is thus associated with a weaker heterolytic BDE leading to CH₃⁺ and :XH.^{12,13}

A closely related rationalization of the effect of protonation on the C–X bond length and BDE comes from noting that there are two major resonance contributors to the C–X bond, namely a covalent (single-bond) structure (**1a**) and an ionic (no-bond) structure (**1b**):



In unprotonated molecules (**1**), the bonded structure (**1a**) dominates, but when a molecule is protonated on X (**2**), the contribution from the no-bond resonance structure (**2b**) can become significant, resulting in lower C–X heterolytic BDEs and longer C–X bonds.

Organic free radicals represent another important class of reactive intermediates. They are more difficult to study experimentally than closed-shell species and there have been comparatively few experimental determinations of free radical structures, heats of formation ($\Delta_f H^\circ$), proton affinities (PA), and radical stabilization energies (RSE). Theory, therefore, has an important role to play in understanding the properties of these species. Protonated forms of $\cdot\text{CH}_2\text{X}$ radicals can have either the CH₃X⁺ or the $\cdot\text{CH}_2\text{XH}^+$ structure. The latter are the so-called distonic radical cations in which the charge and radical sites are formally separated.^{14–16} The distonic ions are more stable than the conventional CH₃X⁺ isomers for the first-row systems, while the latter are preferred for the second-row substituents.¹⁷

The aims of the present study are to compare protonated species with unprotonated species and to compare radicals with the corresponding closed-shell molecules. Specifically, we seek to examine the effects of protonation on the structure, stability, and thermochemistry of organic carbon-centered free radicals using ab initio molecular orbital calculations at the G2 level of theory¹⁸ and to compare the results with those of their closed-shell counterparts. Do the trends observed in BDE and geometry noted above for closed-shell molecules carry over to the open-shell systems? How does the radical center influence the proton affinity at adjacent heteroatoms? How does the effect of a π -donor substituent (e.g., X = NH₂) compare with that of a π -acceptor substituent (e.g., X = CHO)? We have chosen for this study a set of prototypical free radicals, $\cdot\text{CH}_2\text{X}$, substituted with groups X that cover a range of chemical

characteristics, including the halogens (X = F, Cl, and Br), several other first- and second-row π -donor groups (X = NH₂, OH, OCH₃, PH₂, and SH), and several π -acceptor groups (X = CN, CHO, and NO₂).¹⁹ To facilitate comparison of the present results for radicals with those for the protonated forms of the closed-shell CH₃X molecules (CH₃XH⁺), this paper deals only with the distonic forms of the protonated radicals ($\cdot\text{CH}_2\text{XH}^+$).

Computational Methods

Standard ab initio molecular orbital calculations²⁰ were carried out at the G2 level of theory¹⁸ with the use of the GAUSSIAN 92^{21a} and GAUSSIAN 94^{21b} programs. G2 theory corresponds effectively to a QCISD(T)/6-311+G(3df,2p) energy calculation, with the inclusion of zero-point vibrational energy (ZPE) and the incorporation of an empirical higher-level correction (HLC) employed to overcome residual basis set deficiencies. Geometries are optimized at the MP2(full)/6-31G(d) level of theory and zero-point vibrational energies are calculated from HF/6-31G(d) harmonic vibrational frequencies, scaled by 0.8929.¹⁸ Unrestricted open-shell reference wave functions were used for open-shell species throughout the study. The G2 total energies at 298 K, along with $\langle S^2 \rangle$ values (for the underlying UHF/6-31G(d) wave function) for the open-shell systems, are listed in Table S1 of the Supporting Information. Complete geometries of the species dealt with in this study are given in the form of GAUSSIAN archive entries in Table S2 of the Supporting Information.

G2 theory has been employed successfully in calculating proton affinities of closed-shell molecules.²² One problem encountered when studying open-shell systems is spin-contamination in the reference unrestricted Hartree–Fock wave function. In a recent assessment of theoretical procedures for calculating free radical thermochemistry,²³ we concluded that for radicals exhibiting low levels of spin-contamination ($\langle S^2 \rangle \leq 0.80$ compared with 0.75 for a pure doublet state), G2 theory might generally be expected to be adequate for obtaining reliable $\Delta_f H^\circ$ values. Most of the radicals in the present study fall into this category. We also concluded that obtaining reliable $\Delta_f H^\circ$ values for highly spin-contaminated radicals can require a more sophisticated theoretical treatment and we presented details of a recommended procedure.²³ Such a treatment would be expected to lead to improved results for 4 of the 22 radicals under consideration in the present study, namely $\cdot\text{CH}_2\text{CN}$, $\cdot\text{CH}_2\text{CNH}^+$, $\cdot\text{CH}_2\text{CHO}$, and $\cdot\text{CH}_2\text{NO}_2\text{H}^+$, but we have not included calculations of this type here.

Proton affinities at 0 K have been evaluated from G2 total energies as the negative of the energy changes for reaction 1. We note that G2 PAs are completely ab initio since the HLC in G2 theory is the same on both sides of the protonation reaction. To obtain theoretical PAs at 298 K, vibrational contributions to thermal corrections^{19,24} were calculated with the use of HF/6-31G(d) harmonic frequencies, scaled by 0.8929 according to the G2 scheme.¹⁸ Theoretical heats of formation

(19) The effect of protonation on the $\cdot\text{CH}_2\text{OH}$ radical has been discussed in a recent study that also examines the $\cdot\text{CH}_2\text{CH}_2\text{OH}$ and $\cdot\text{CH}_2\text{CH}_2\text{CH}_2\text{OH}$ systems: Gauld, J. W.; Holmes, J. L.; Radom, L. *Acta Chem. Scand.* **1997**, *51*, 641.

(20) Hehre, W. J.; Radom, L.; Schleyer, P. v. R.; Pople, J. A. *Ab Initio Molecular Orbital Theory*; Wiley: New York, 1986.

(21) (a) Frisch, M. J.; Trucks, G. W.; Head-Gordon, M.; Gill, P. M. W.; Wong, M. W.; Foresman, J. B.; Johnson, B. G.; Schlegel, H. B.; Robb, M. A.; Replegle, E. S.; Gomperts, R.; Andres, J. L.; Raghavachari, K.; Binkley, J. S.; Gonzalez, C.; Martin, R. L.; Fox, D. J.; DeFrees, D. J.; Baker, J.; Stewart, J. J. P.; Pople, J. A. GAUSSIAN 92, Gaussian Inc.: Pittsburgh, PA, 1992. (b) Frisch, M. J.; Trucks, G. W.; Schlegel, H. B.; Gill, P. M. W.; Johnson, B. G.; Robb, M. A.; Cheeseman, J. R.; Keith, T.; Petersson, G. A.; Montgomery, J. A.; Raghavachari, K.; Al-Laham, M. A.; Zakrewski, V. G.; Ortiz, J. V.; Foresman, J. B.; Cioslowski, J.; Stefanov, B. B.; Nanayakkara, A.; Challacombe, M.; Peng, C. Y.; Ayala, P. Y.; Chen, W.; Wong, M. W.; Andres, J. L.; Replegle, E. S.; Gomperts, R.; Martin, R. L.; Fox, D. J.; Binkley, J. S.; DeFrees, D. J.; Baker, J.; Stewart, J. J. P.; Head-Gordon, M.; Gonzalez C.; Pople, J. A. GAUSSIAN 94; Gaussian Inc.: Pittsburgh, PA, 1995.

(22) For a detailed study, see: Smith, B. J.; Radom, L. *J. Am. Chem. Soc.* **1993**, *115*, 4885.

(23) Mayer, P. M.; Parkinson, C. J.; Smith, D. M.; Radom, L. *J. Chem. Phys.* In press.

(24) Daudel, R.; Leroy, G.; Peeters, D.; Sana, M. *Quantum Chemistry*; Wiley: New York, 1983.

(14) (a) Radom, L.; Bouma, W. J.; Nobes, R. H.; Yates, B. F. *Pure Appl. Chem.* **1984**, *56*, 1831. (b) Yates, B. F.; Bouma, W. J.; Radom, L. *Tetrahedron* **1986**, *42*, 6225. (c) Yates, B. F.; Bouma, W. J.; Radom, L. *J. Am. Chem. Soc.* **1987**, *109*, 2250.

(15) Hammerum, S. *Mass Spectrom. Rev.* **1988**, *7*, 123.

(16) Stirk, K. M.; Kiminkinen, L. K. M.; Kenttämäa, H. *Chem. Rev.* **1992**, *92*, 1649.

(17) For a discussion of the relative stabilities of CH₃X⁺ and $\cdot\text{CH}_2\text{XH}^+$ structures calculated at the G2 level, see: Gauld, J. W.; Radom, L. *J. Phys. Chem.* **1994**, *98*, 777.

(18) (a) Curtiss, L. A.; Raghavachari, K.; Trucks, G. W.; Pople, J. A. *J. Chem. Phys.* **1991**, *94*, 7221. (b) Curtiss, L. A.; McGrath, M. P.; Blaudeau, J.-P.; Davis, N. E.; Binning, R. C., Jr.; Radom, L. *J. Chem. Phys.* **1995**, *103*, 6104. For reviews of the applications of G2 theory, see: (c) Curtiss, L. A.; Raghavachari, K. *Quantum Mechanical Electronic Structure Calculations with Chemical Accuracy*, Langhoff, S. R., Ed.; Kluwer Academic Press: The Netherlands, 1995. (d) Raghavachari, K.; Curtiss, L. A. *Modern Electronic Structure Theory*; Yarkony, D. R., Ed.; World Scientific: Singapore, 1995.

Table 1. Optimized C–X and C–XH⁺ Bond Lengths in the Substituted Methanes (CH₃X), Methyl Radicals ([•]CH₂X), and Their Protonated Forms (CH₃XH⁺ and [•]CH₂XH⁺)^{a,b}

	r(C–X)	r(C–XH ⁺)
CH ₃ –NH ₂	1.465 (1.471)	1.508
[•] CH ₂ –NH ₂	1.402	1.471
CH ₃ –OH	1.424 (1.429)	1.516
[•] CH ₂ –OH	1.373	1.468
CH ₃ –OCH ₃	1.414 (1.415)	1.494
[•] CH ₂ –OCH ₃	1.363	1.437
CH ₃ –F	1.390 (1.383)	1.603
[•] CH ₂ –F	1.350	1.550
CH ₃ –PH ₂	1.860 (1.858)	1.800
[•] CH ₂ –PH ₂	1.790	1.764
CH ₃ –SH	1.814 (1.814)	1.818
[•] CH ₂ –SH	1.728	1.762
CH ₃ –Cl	1.778 (1.776)	1.845
[•] CH ₂ –Cl	1.718	1.773
CH ₃ –Br	1.949 (1.934)	2.001
[•] CH ₂ –Br	1.863	1.925
CH ₃ –CN	1.461 (1.468)	1.448
[•] CH ₂ –CN	1.412	1.407
CH ₃ –CHO	1.502 (1.501)	1.457
[•] CH ₂ –CHO	1.456	1.408
CH ₃ –NO ₂	1.486 (1.489)	1.480
[•] CH ₂ –NO ₂	1.431	1.330

^a MP2(full)/6-31G(d) values, in Å. ^b Experimental values in parentheses from ref 27.

at 0 K ($\Delta_f H^\circ_0$) were derived from the G2 energies by the atomization method as outlined by Nicolaides et al.²⁵ and using the experimental heats of formation of the atoms.³ Heats of formation at 298 K ($\Delta_f H^\circ_{298}$) were evaluated with the use of calculated thermal corrections for the species of interest together with the experimental enthalpy increments ($H^\circ_{298} - H^\circ_0$) of the elements in their standard states.²⁶

Results and Discussion

Changes in C–X Bond Length in Going from CH₃X to [•]CH₂X. The C–X bond lengths for the substituted methanes (CH₃X) and substituted methyl radicals ([•]CH₂X) are listed in Table 1. There is close agreement between the theoretical values and available experimental data,²⁷ despite the fairly simple level of theory used (MP2/6-31G(d)). The mean absolute difference between theoretical and experimental bond lengths is just 0.004 Å.

An important observation is that in all cases the C–X bond is significantly shorter in the radicals than in their closed-shell counterparts. This result can be rationalized by noting that hyperconjugative interaction between the CH₃ group and X in CH₃X is not as strong as the interaction between [•]CH₂ and X in [•]CH₂X. In the case of π -donor substituents, the hyperconjugative interaction in CH₃X takes the form of donation from the lone pair on X, n(X), to an antibonding orbital of π -symmetry on the methyl group, $\pi^*(\text{CH}_3)$.²⁸ For the π -acceptor substituents (X = CN, HCO and NO₂), hyperconjugative donation takes place from a $\pi(\text{CH}_3)$ orbital to a π^* orbital on X.²⁸ For the π -donor-substituted methyl radicals, overlap

(25) Nicolaides, A.; Rauk, A.; Glukhovtsev, M. N.; Radom, L. *J. Phys. Chem.* **1996**, *100*, 17460.

(26) Wagman, D. D.; Evans, W. H.; Parker, V. B.; Schumm, R. H.; Halow, I.; Bailey, S. M.; Churney, K. L.; Nuttall, R. L. *J. Phys. Chem. Ref. Data* **1982**, *11*, Suppl. 2.

(27) Values taken from the following: Structure Data of Free Polyatomic Molecules. *Landolt-Börnstein, New Series*; Vol. II/23 (polyatomic molecules): Kuchitsu, K., Ed.; 1995, and earlier compendia in the series as referenced in II/23.

(28) See, for example: Radom, L. *Prog. Theor. Org. Chem.* **1981**, *3*, 1.

Table 2. Comparison of Calculated (G2) and Experimental Electron Affinities of X and Ionization Energies of XH, CH₃, and CH₂

X	EA(X) ^a		XH	IE(XH) ^b	
	G2 ^c	exptl ^d		G2 ^c	exptl ^d
NH ₂	0.77	0.75 ± 0.06	NH ₃	10.19	10.16 ± 0.01
OH	1.87	1.829 ± 0.010	H ₂ O	12.63	12.612 ± 0.010
CH ₃ O	1.62	1.62 ± 0.14	CH ₃ OH	10.97	10.85 ± 0.01
F	3.48	3.399 ± 0.003	HF	16.08	16.004 ± 0.003
PH ₂	1.25	1.19 ± 0.14	PH ₃	9.87	9.869 ± 0.002
SH	2.30	2.32 ± 0.10	H ₂ S	10.43	10.453 ± 0.008
Cl	3.61	3.617 ± 0.003	HCl	12.71	12.747
Br	3.10	3.365 ± 0.003	HBr	11.58	11.66 ± 0.03
CN	3.97	3.74 ± 0.17	CNH	12.06	12.5 ± 0.1
CHO	0.34	0.313 ± 0.005	CHOH	8.95	
NO ₂	2.34	2.30 ± 0.10	NO ₂ H	10.98	
			CH ₃	9.77	9.84 ± 0.01
			CH ₂	10.31	10.396

^a Energies for the reaction X[•] → X⁻, in eV, at 0 K. ^b Energies for the reaction XH → XH⁺, in eV, at 0 K. ^c Many of these values can also be found in Curtiss et al.^{18a,b} ^d Lias et al.³

between the formally singly-occupied orbital at C ($p(\text{C})$) and $n(\text{X})$ is possible, leading to a net-bonding three-electron interaction.^{28–30} This is generally a more favorable interaction than the hyperconjugation in CH₃X, thereby shortening the C–X bond.²⁸ For X = CN, HCO, and NO₂, more effective delocalization of the unpaired electron through a three-center three-electron interaction means that the C–X bond in [•]CH₂X will have greater partial-double-bond character than in CH₃X, again leading to a relative bond shortening.

Changes in C–X Bond Length Due to Protonation at X.

The changes in C–X bond length in CH₃X and [•]CH₂X following protonation at X are compared in Table 1. Our MP2(full)/6-31G(d) geometries are essentially identical with the MP2/6-31G(d) geometries calculated by Boyd et al.¹¹ for X = NH₂, OH, and F, and are similar to their MP2/6-31+G(d,p) results for X = PH₂, SH, and Cl.¹³ For the π -donor substituents X, the C–X bond lengths in the substituted methanes generally increase with protonation, sometimes quite markedly, as observed previously by Yáñez⁹ and Boyd.^{11–13} Protonation of the π -donor group X serves to reduce the hyperconjugative electron donation from X to the $\pi^*(\text{CH}_3)$ orbital, thereby reducing the extent of double-bond character in the C–X bond. Also, as noted above, protonation of the heteroatom serves to increase the contribution of the no-bond resonance structure, ⁺CH₃:XH (**2b**), to the C–X bond. This behavior can be readily understood from a consideration of the electron affinities (EA) of X and ionization energies (IE) of XH (Table 2). In the unprotonated molecule (CH₃X), the C–X bond is best described by the bonded resonance structure **1a** because the IE of [•]CH₃ is considerably greater than the EA of X. The two electrons forming the bond will be shared by the CH₃ group and X, thus making the no-bond resonance structure **1b** relatively unimportant. In the protonated molecule (CH₃XH⁺), the IE of XH becomes comparable to, or in some cases (e.g., X = F) much greater than, the IE of [•]CH₃. This increases the contribution of the no-bond resonance structure **2b** to the C–X bond, resulting in a longer bond length than in the unprotonated species. The only exception to this behavior occurs for the PH₂ substituent.

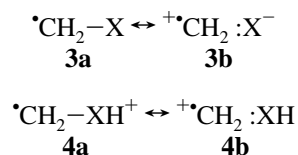
(29) Leroy, G.; Peeters, D.; Sana, M.; Wilante, C. In *Substituent Effects in Radical Chemistry*; Viehe, H. G., Janousek, Z., Merényi, R., Eds.; D. Reidel: Dordrecht, 1986; p 1.

(30) (a) Bernardi, F.; Epiotis, N. D.; Cherry, W.; Schlegel, H. B.; Whangbo, M.-H.; Wolfe, S. J. *Am. Chem. Soc.* **1976**, *98*, 469. (b) Bernardi, F.; Epiotis, N. D. In *Applications of Molecular Orbital Theory in Organic Chemistry*; Csizmadia, I. G., Ed.; Elsevier: Amsterdam, 1977; p 47. (c) Crans, D.; Clark, T.; Schleyer, P. v. R. *Tetrahedron Lett.* **1980**, *21*, 3681.

In this case, because the IE of PH₃ is only slightly greater than that of [•]CH₃ (9.87 eV vs 9.77 eV) (Table 2), the character of the C–P bond in CH₃–PH₃⁺ will still be dominated by the bonded resonance structure (**2a**), leading to a C–P bond length that is shorter than in CH₃–PH₂.

The molecules with π-acceptor substituents (X = CN, CHO, and NO₂) all exhibit shortening of the C–X bond upon protonation. In the unprotonated species, hyperconjugative donation from a π(CH₃) orbital to a π*(X) orbital strengthens the C–X bond. Protonation of X lowers the energy of the π*(X) orbital, thereby enhancing the extent of the hyperconjugative interaction with π(CH₃). This generally leads to a further shortening of the C–X bond relative to that in the unprotonated species. In cases where XH has a large ionization energy (e.g., X = CN), the opposing effect of an increased contribution from the no-bond resonance structure **2b** becomes important so that the overall effect is quite small.

Similar arguments can be used to rationalize the effect of protonation on the C–X bond lengths in the [•]CH₂X radicals (Table 1). The C–X bonds can again be described as having two major resonance contributors:



As with the closed-shell species, the unprotonated radicals [•]CH₂X bearing π-donor substituents X are dominated by the bonded resonance structure **3a**. Following protonation, however, there is an increase in the contribution of the no-bond resonance structure **4b** to the description of the C–X bond in such radicals because the XH molecules have ionization energies similar to or even higher than that of CH₂. There is a consequent increase in the C–X bond length. The only exception to this trend again occurs for X = PH₂, arising because the IE of PH₃ is considerably lower than that of CH₂. This results in the bonded resonance structure **4a** remaining the dominant contributor to the C–P bond.

The π-acceptor substituents CN, CHO, and NO₂ all permit efficient delocalization of the unpaired electron in [•]CH₂X and thus the C–X bond in each case will have partial-double-bond character. This conjugative interaction is enhanced following protonation and as a result the C–X bond is shortened (as was also noted for the closed-shell systems).

Changes in C–X Bond Length vs X. The changes in C–X bond lengths across the first and second rows of the periodic table show opposite behavior depending on whether the molecules are unprotonated or protonated (Table 1). For the unprotonated molecules (CH₃X), the C–X bond gets shorter as one goes from left to right in the table, whereas for the protonated molecules (CH₃XH⁺) the C–X bond lengthens. The shortening of the C–X bond across the first- and second-row substituents in neutral CH₃X molecules is well established and has been rationalized previously on the basis of electronegativity arguments:^{9–13} the C–X bond shortens as the difference in electronegativity between CH₃ and X increases, i.e., the bond lengths are in the order X = NH₂ > OH > F and X = PH₂ > SH > Cl. For protonated molecules CH₃XH⁺, the no-bond resonance structure **2b** becomes more important and the C–X bond length will increase as the contribution of this nonbonded structure increases. This contribution in turn will become more significant as the IE of XH increases. Thus, the C–X length will increase in the order X = NH₂ < OH < F and X = PH₂ < SH < Cl (Table 1).

Table 3. Calculated Homolytic and Heterolytic BDEs of CH₃X, [•]CH₂X, and Their Protonated Counterparts

	homolytic BDE ^a		heterolytic BDE ^a	
	C–X	C–XH ⁺	C–X	C–XH ⁺
CH ₃ NH ₂	358.2	478.4	1226.3	437.7
[•] CH ₂ NH ₂	429.8	483.5	1350.3	495.1
CH ₃ OH	391.5	552.7	1153.5	277.0
[•] CH ₂ OH	450.2	552.3	1264.4	328.8
CH ₃ OCH ₃	359.4	452.6	1145.4	336.7
[•] CH ₂ OCH ₃	418.3	456.9	1256.6	393.2
CH ₃ F	470.1	733.0	1077.3	123.7
[•] CH ₂ F	507.6	707.2	1167.1	150.3
CH ₃ PH ₂	302.3	449.7	1124.7	440.2
[•] CH ₂ PH ₂	352.7	468.9	1227.4	511.7
CH ₃ SH	313.4	401.0	1034.0	337.5
[•] CH ₂ SH	376.3	413.4	1149.2	402.2
CH ₃ Cl	353.6	483.6	948.8	199.6
[•] CH ₂ Cl	399.1	481.2	1046.6	249.4
CH ₃ Br	292.8	397.5	936.7	223.1
[•] CH ₂ Br	333.1	396.8	1029.3	274.7
CH ₃ CN	520.3	676.5	1079.6	455.2
[•] CH ₂ CN	578.0	714.9	1189.7	546.0
CH ₃ CHO	357.0	522.9	1267.2	602.0
[•] CH ₂ CHO	418.5	593.3	1380.9	724.8
CH ₃ NO ₂	263.6	420.4	980.2	303.8
[•] CH ₂ NO ₂	300.4	464.8	1069.2	400.5

^a At 298 K in kJ mol⁻¹.

The results for the unprotonated free radicals [•]CH₂X follow the trend set by their closed-shell counterparts, i.e., the C–X bond gets shorter as the electronegativity of X increases. The protonated free radicals [•]CH₂XH⁺, however, show bond length changes that reflect two competing effects: first, the intrinsic tendency for the C–X bond to shorten as XH becomes more electronegative, and second, the tendency for the C–X bond to lengthen as the contribution of the no-bond structure **4b** increases, i.e., as the IE of XH increases. The net result of these two effects is a very slight shortening of the C–X bond in going from X = NH₂ to OH and from PH₂ to SH (by 0.003 and 0.002 Å, respectively), followed by a lengthening of the bond for the halogen substituents. It appears that the added significance of the nonbonded resonance structures in the two protonated free radicals [•]CH₂OH₂⁺ and [•]CH₂SH₂⁺ is insufficient to overcome the electronegativity increase of the XH group, resulting in the slight calculated bond shortening compared with [•]CH₂NH₃⁺ and [•]CH₂PH₃⁺.

Changes in C–X BDE Due to Protonation at X. The homolytic and heterolytic bond dissociation enthalpies (BDEs) for the C–X bond in the substituted methanes, methyl radicals, and their protonated counterparts, calculated at the G2 level of theory, are listed in Table 3. The most striking observation from Table 3 is the dramatic drop in heterolytic BDE for the protonated species. This behavior has been observed previously for the closed-shell systems by Boyd et al.^{11–13} Heterolytic cleavage of a C–X bond in a protonated molecule CH₃XH⁺ does not result in the unfavorable charge separation that occurs for a neutral molecule CH₃X, and thus is associated with a smaller heterolytic BDE. The effect will be largest for substituents XH having large IEs. Indeed, the lowest heterolytic BDE for protonated closed-shell species is exhibited by CH₃–FH⁺ and for protonated free radicals by [•]CH₂FH⁺ (Table 3).

The homolytic C–X BDEs exhibit the opposite trend to the heterolytic values, i.e., they tend to increase upon protonation. This behavior for closed-shell species has been rationalized by Yáñez et al.^{8–10} and Boyd et al.^{11–13} in terms of the increased

Table 4. Comparison of Calculated and Experimental Radical Stabilization Energies for $\cdot\text{CH}_2\text{X}$ Radicals and Their Protonated Forms, $\cdot\text{CH}_2\text{XH}^+$ ^a

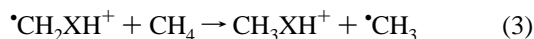
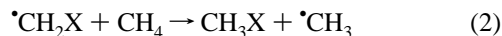
X	RSE($\cdot\text{CH}_2\text{X}$)		RSE($\cdot\text{CH}_2\text{XH}^+$)
	G2	exptl ^b	G2
NH ₂	46.9	38.3 ± 9 ^c	-19.7
OH	33.9	35.3 ± 7 ^d	-25.2
OCH ₃	34.1	50 ± 5	-20.5
F	12.7	6.3 ± 9	-50.6
PH ₂	25.6		-5.6
SH	38.1	49.1 ± 10 ^e	-12.4
Cl	20.7	21.0 ± 4.1 ^f	-27.2
Br	15.5	8 ± 3	-25.5
CN	33.0	50 ± 11	13.7
CHO	36.7		45.7
NO ₂	12.0		19.6

^a Enthalpies for the reactions 2 and 3, respectively, at 298 K in kJ mol⁻¹. ^b Using values from Lias et al.³ unless otherwise stated. ^c Griller and Lossing³⁴ give 41.4 kJ mol⁻¹ while Bordwell et al.³⁵ give 43.1 kJ mol⁻¹. ^d Using $\Delta_f H_{298}^\circ(\cdot\text{CH}_2\text{OH}) = -16.6 \pm 0.9$ kJ mol⁻¹ (Ruscic and Berkowitz).³⁶ ^e Using $\Delta_f H_{298}^\circ(\cdot\text{CH}_2\text{SH}) = 150.0 \pm 8.4$ kJ mol⁻¹ (Ruscic and Berkowitz).³⁷ ^f Using $\Delta_f H_{298}^\circ(\cdot\text{CH}_2\text{Cl}) = 117.3 \pm 3.1$ kJ mol⁻¹ (Seetula).³⁸

electronegativity of the X group following protonation: the homolytic BDE of CH₃X increases upon protonation of X since protonation increases the electronegativity difference between CH₃ and X.

In many of the cases in Table 3, the heterolytic BDEs in the protonated molecules and protonated free radicals are actually lower than the corresponding homolytic BDEs. This is a consequence of the added importance of the no-bond resonance structures $\cdot\text{CH}_3:\text{XH}$ and $\cdot\text{CH}_2:\text{XH}$ in describing the C-X bond. As was observed for the C-X bond lengths, however, there are a small number of cases in which this does not occur, specifically $\cdot\text{CH}_2\text{NH}_3^+$, $\cdot\text{CH}_2\text{PH}_3^+$, CH_3CHOH^+ , and $\cdot\text{CH}_2\text{-CHOH}^+$. In each of these cases, the IE of XH (XH = NH₃, PH₃, or CHOH, see Table 2) is similar to or lower than that of CH₃ or CH₂, and hence the C-X bonds in these systems are still influenced to a large extent by the bonded resonance structure.

Stabilization Energies of the $\cdot\text{CH}_2\text{X}$ Radicals and Their Protonated Forms $\cdot\text{CH}_2\text{XH}^+$. To evaluate the effect of substituents on the stability of the $\cdot\text{CH}_2\text{X}$ radicals and their X-protonated forms, we have calculated radical stabilization energies (RSEs),^{19,29,31-33} as defined by the enthalpy changes for the following isodesmic reactions:



The calculated RSEs are compared with available experimental values³⁴⁻³⁸ in Table 4. Agreement between theoretical and experimental RSEs is generally quite reasonable but discrepancies of up to 17 kJ mol⁻¹ may be seen. We note that the

(31) Leroy, G.; Sana, M.; Wilante, C.; Nemba, R. M. *J. Mol. Struct.* **1989**, *198*, 159.

(32) Pasto, D. J.; Krasnansky, R.; Zercher, C. *J. Org. Chem.* **1987**, *52*, 3062.

(33) Hawari, J. A.; Kanabus-Kaminska, J. M.; Wayner, D. D. M.; Griller, D. In *Substituent Effects in Radical Chemistry*; Viehe, H. G., Janousek, Z., Merényi, R., Eds.; D. Reidel: Dordrecht, 1986; p 91.

(34) Griller, D.; Lossing, F. P. *J. Am. Chem. Soc.* **1981**, *103*, 1586.

(35) (a) Bordwell, F. G.; Zhang, X.-M.; Alnajjar, M. S. *J. Am. Chem. Soc.* **1992**, *114*, 7623. (b) Bordwell, F. G.; Lynch, T.-Y. *J. Am. Chem. Soc.* **1989**, *111*, 7558.

(36) Ruscic, B.; Berkowitz, J. J. *Phys. Chem.* **1993**, *97*, 11451.

(37) Ruscic, B.; Berkowitz, J. J. *Chem. Phys.* **1992**, *97*, 1818.

(38) Seetula, J. A. *J. Chem. Soc., Faraday Trans.* **1996**, *92*, 3069.

Table 5. Comparison of Calculated and Experimental C-H Bond Dissociation Enthalpies in CH₃X and CH₃XH⁺^a

X	BDE(H-CH ₂ X)		BDE(H-CH ₂ XH ⁺)
	G2	exptl ^b	G2
H	442.6	438.3	
NH ₂	395.7	400.0 ± 8.4	462.2
OH	408.7	403 ± 2 ^c	467.8
OCH ₃	408.5	389 ± 4	463.1
F	429.9	432.0 ± 8.4	493.1
PH ₂	417.0		448.2
SH	404.5	390.9 ± 8.4 ^d	455.0
Cl	421.9	417.3 ± 3.1 ^e	469.8
Br	427.0	430 ± 1	468.1
CN	409.6	389 ± 10	428.9
CHO	405.9		396.9
NO ₂	430.6	407.5 ^f	422.9

^a In kJ mol⁻¹ at 298 K. ^b Using $\Delta_f H_{298}^\circ$ values from Lias et al.³ unless otherwise stated. ^c Using $\Delta_f H_{298}^\circ(\cdot\text{CH}_2\text{OH}) = -16.6 \pm 0.9$ kJ mol⁻¹ (Ruscic and Berkowitz).³⁶ ^d Using $\Delta_f H_{298}^\circ(\cdot\text{CH}_2\text{SH}) = 150.0 \pm 8.4$ kJ mol⁻¹ (Ruscic and Berkowitz).³⁷ ^e Using $\Delta_f H_{298}^\circ(\cdot\text{CH}_2\text{Cl}) = 117.3 \pm 3.1$ kJ mol⁻¹ (Seetula).³⁸ ^f Bordwell and Satish.⁴⁰

experimental uncertainties are not insignificant and that, for strongly spin-contaminated systems (e.g., X = CN), the G2 values may be less reliable than normal.²³

Factors governing the stabilization of $\cdot\text{CH}_2\text{X}$ radicals are well documented,^{29-31,33,39} and include the n(X) → p(C) interaction when X is a π-donor substituent, and delocalization of the unpaired electron when X is a π-acceptor substituent.²⁸⁻³⁰

The RSEs for the protonated radicals with π-donor substituents are all negative, i.e., the stabilization is less in the $\cdot\text{CH}_2\text{-XH}^+$ radicals than in CH₃XH⁺ (Table 4). Protonation of X produces a smaller n(X) → p(C) interaction because of the lowering in energy of the lone-pair orbital. For the π-acceptor substituents (X = CN, HCO, and NO₂), delocalization of the unpaired electron is enhanced in the protonated forms of the radicals, and hence $\cdot\text{CH}_2\text{XH}^+$ are stabilized to a greater extent than CH₃XH⁺.

The absolute C-H BDE values in CH₃X and CH₃XH⁺ are listed in Table 5. For all the π-donor substituents and CN, the C-H BDEs are larger for the protonated species than for the unprotonated species, whereas for X = CHO and NO₂, the reverse is true.

Proton Affinities of CH₃X and $\cdot\text{CH}_2\text{X}$. Calculated G2 gas-phase proton affinities (PAs) of CH₃X and $\cdot\text{CH}_2\text{X}$ are listed in Table 6. Agreement with the values quoted in Lias et al.³ is quite variable, but there is considerable improvement when more recent experimental values are used, such as those of Szulejko and McMahon^{5,44} and Audier and co-workers,^{42,43} or those listed in a recent compendium by Hunter and Lias.⁷

Comparison of the PAs of $\cdot\text{CH}_2\text{X}$ radicals with the PAs of the corresponding CH₃X molecules shows that for π-donor substituents, the proton affinities are 30-70 kJ mol⁻¹ lower in the radicals than in the corresponding closed-shell molecules (Table 6). This behavior may be rationalized by noting that the n(X) → p(C) interaction in the radicals makes the lone pair

(39) (a) Sana, M.; Leroy, G. *J. Mol. Struct. (Theochem)* **1991**, *226*, 307.

(b) Leroy, G.; Sana, M.; Wilante, C. *J. Mol. Struct. (Theochem)* **1991**, *228*, 37. (c) Sana, M.; Leroy, G.; Hilali, M.; Nguyen, M. T.; Vanquickenborne, L. G. *Chem. Phys. Lett.* **1992**, *190*, 551.

(40) Bordwell, F. G.; Satish, A. V. *J. Am. Chem. Soc.* **1994**, *116*, 8885.

(41) (a) Fox, G. L.; Schlegel, H. B. *J. Phys. Chem.* **1992**, *96*, 298. (b) Walch, S. P. *J. Chem. Phys.* **1993**, *98*, 3076.

(42) Audier, H. E.; Fossey, J.; Mourgues, P.; Leblanc, D.; Hammerum, S. *Int. J. Mass Spectrom. Ion Proc.* **1996**, *157/158*, 275.

(43) Mourgues, P.; Audier, H. E.; Leblanc, D.; Hammerum, S. *Org. Mass Spectrom.* **1993**, *28*, 1098.

(44) Glukhovtsev, M. N.; Szulejko, J. E.; McMahon, T. B.; Gauld, J. W.; Scott, A. P.; Smith, B. J.; Pross, A.; Radom, L. *J. Phys. Chem.* **1994**, *98*, 13099.

Table 6. Comparison of Calculated and Experimental Proton Affinities^a of Substituted Methanes and Substituted Methyl Radicals

	PA			
	G2	Lias et al. ^b	Hunter and Lias ^c	other data
CH ₃ NH ₂	900.9	896	899	901.2 ^d
•CH ₂ NH ₂	834.3	>848 ± 8	849.4	>839.6, ^e 829 ^f
CH ₃ OH	753.2	761	754.3	760.2 ^d
•CH ₂ OH	695.3		695	695 ± 8, ^g 695 ± 4, ^f 698 ± 9 ^h
CH ₃ OCH ₃	792.0	804	792.0	793.3 ^d
•CH ₂ OCH ₃	739.9		756.1	751 ± 6 ^f
CH ₃ F	597.6	605	598.8	597.1 ⁱ
•CH ₂ F	534.3	589 ± 8		532 ± 23 ^j
CH ₃ PH ₂	855.0	854	852.0	
•CH ₂ PH ₂	823.8			797 ± 13 ^k
CH ₃ SH	776.3	784	773.4	
•CH ₂ SH	725.8		735.1	764 ± 8, ^l <732.2 ^m
CH ₃ Cl	649.7	682	648.2	650.6 ^l
•CH ₂ Cl	601.1	631		605 ⁿ
CH ₃ Br	663.3	693	664.2	662.3 ⁱ
•CH ₂ Br	622.3	714		
CH ₃ CN	780.1	817	779.2	
•CH ₂ CN	763.0			
CH ₃ CHO	770.2	781	769.1	
•CH ₂ CHO	779.8		774.0	
CH ₃ NO ₂	745.6		752.8	
•CH ₂ NO ₂	752.1			

^a Values given correspond to protonation at X, at 298 K in kJ mol⁻¹.
^b Either listed in, or derived using $\Delta_f H^\circ_{298}$ values from Lias et al.³
^c Values listed by Hunter and Lias.⁷ ^d Szulejko and McMahon.⁵ ^e Using $\Delta_f H^\circ_{298}(\text{CH}_2\text{NH}_2) = 150.6$ kJ mol⁻¹ (Griller and Lossing)³⁴ and $\Delta_f H^\circ_{298}(\text{CH}_2\text{NH}_3^+) \leq 841$ kJ mol⁻¹ (Lias et al.).³ ^f Audier et al.⁴²
^g Mourgues et al.⁴³ ^h Using $\Delta_f H^\circ_{298}(\text{CH}_2\text{OH}) = -16.6 \pm 0.9$ kJ mol⁻¹ (Ruscic and Berkowitz).³⁶ ⁱ Glukhovtsev et al.⁴⁴ ^j Calculated using $\Delta_f H^\circ_{298}(\text{CH}_2\text{FH}^+) = 965 \pm 15$ kJ mol⁻¹ (J. L. Holmes, private communication, cited by Gauld et al.)¹⁷ and $\Delta_f H^\circ_{298}(\text{CH}_2\text{F}) = -33 \pm 8$ kJ mol⁻¹ (Lias et al.).³ ^k Schweighofer et al.⁴⁵ ^l Using $\Delta_f H^\circ_{298}(\text{CH}_2\text{SH}) = 150.0 \pm 8.4$ kJ mol⁻¹ (Ruscic and Berkowitz)³⁷ and $\Delta_f H^\circ_{298}(\text{CH}_2\text{SH}_2^+) = 916$ kJ mol⁻¹ (Lias et al.).³ ^m Chou et al.⁴⁶ ⁿ Using $\Delta_f H^\circ_{298}(\text{CH}_2\text{Cl}) = 117.3 \pm 3.1$ kJ mol⁻¹ (Seetula)³⁸ and $\Delta_f H^\circ_{298}(\text{CH}_2\text{ClH}^+) = 1029$ kJ mol⁻¹ (Lias et al.).³

less available for protonation. For the •CH₂CHO and •CH₂-NO₂ radicals, the orbital that accepts the incoming proton lies in the plane of the radicals and is relatively unaffected by the change in going from CH₃X to •CH₂X.

Heats of Formation. We compare the calculated G2 heats of formation for the CH₃X, CH₃XH⁺, •CH₂X, and •CH₂XH⁺ systems with available experimental data in Table 7. Closely related values for some of these systems have been reported elsewhere.¹⁷ The agreement between theory and the most recent experimental values is generally reasonable with 25 of the 38

(45) Schweighofer, A.; Chou, P. K.; Thoen, K. K.; Nanayakkara, V. J.; Keck, H.; Kuchen, W.; Kenttämaa, H. I. *J. Am. Chem. Soc.* **1996**, *118*, 11893.

(46) Chou, P. K.; Smith, R. L.; Chyall, L. J.; Kenttämaa, H. I. *J. Am. Chem. Soc.* **1995**, *117*, 4374.

(47) Armstrong, D. A.; Rauk, A.; Yu, D. *J. Am. Chem. Soc.* **1993**, *115*, 666.

(48) Dóbe, S.; Bérces, T.; Turányi, T.; Márta, F.; Grussdorf, J.; Temps, F.; Wagner, H. G. *J. Phys. Chem.* **1996**, *100*, 19864.

(49) Good, D. A.; Francisco, J. S. *Chem. Phys. Lett.* **1997**, *266*, 512.

(50) Holmes, J. L.; Lossing, F. P. *Int. J. Mass Spectrom. Ion Proc.* **1984**, *58*, 113.

(51) Espinosa-Garcia, J. *Chem. Phys. Lett.* **1996**, *250*, 71.

(52) Pickard, J. M.; Rodgers, A. S. *Int. J. Chem. Kinet.* **1983**, *15*, 569.

(53) Holmes, J. L.; Lossing, F. P. *J. Am. Chem. Soc.* **1988**, *110*, 7343.

(54) Ferguson, K. C.; Okafo, E. N.; Whittle, E. J. *Chem. Soc., Faraday Trans. 1* **1973**, *69*, 295.

(55) Holmes, J. L.; Mayer, P. M. *J. Phys. Chem.* **1995**, *99*, 1366.

(56) Matimba, H. E. K.; Crabbendam, A. M.; Ingemann, S.; Nibbering, N. M. M. *Int. J. Mass Spectrom. Ion Proc.* **1992**, *114*, 85.

Table 7. Comparison of Calculated and Experimental Heats of Formation^a

	$\Delta_f H^\circ_{298}$		
	G2	Lias et al. ³	other exptl data
CH ₃ NH ₂	-22.8	-23.0 ± 0.4	
CH ₃ NH ₃ ⁺	606.9	611	
•CH ₂ NH ₂	154.3 ^b	159 ± 8	150.6 ^c
•CH ₂ NH ₃ ⁺	851.2	<841	
CH ₃ OH	-206.7	-201.6 ± 0.2	
CH ₃ OH ₂ ⁺	568.6	567	
•CH ₂ OH	-16.0	-25.9 ± 6	-16.6 ± 0.9, ^d -16.6 ± 1.3 ^e
•CH ₂ OH ₂ ⁺	819.5	815 ± 8	818.4 ± 4 ^f
CH ₃ OCH ₃	-192.4	-184.0 ± 0.5	g
(CH ₃) ₂ OH ⁺	546.3	542	
•CH ₂ OCH ₃	-2.0	-13 ± 4	-5.4 ± 8, ^{g,h}
•CH ₂ O(H ⁺)CH ₃	791.4		
CH ₃ F	-244.5	-247.0	i
CH ₃ FH ⁺	688.7	678	686 ^j
•CH ₂ F	-32.6	-33 ± 8	-31.8 ± 8.4 ^k
•CH ₂ FH ⁺	963.8	908.0	965 ± 15 ^l
CH ₃ PH ₂	-19.4	-18	
CH ₃ PH ₃ ⁺	656.4	658	
•CH ₂ PH ₂	179.6		
•CH ₂ PH ₃ ⁺	886.6		908 ± 13 ^m
CH ₃ SH	-20.4	-22.9 ± 0.6	
CH ₃ SH ₂ ⁺	733.9	723	
•CH ₂ SH	166.1		150.0 ± 8.4 ⁿ
•CH ₂ SH ₂ ⁺	970.9	916	> 950 ^o
CH ₃ Cl	-84.6	-82.0	
CH ₃ ClH ⁺	796.2	767	798 ^j
•CH ₂ Cl	118.4	130	117.3 ± 3.1, ^p 116 ± 8 ^q
•CH ₂ ClH ⁺	1048.0	1029.0	
CH ₃ Br	-34.0	-38.1 ± 1.3	-34.3 ± 0.8 ^r
CH ₃ BrH ⁺	833.5	800	831 ^j
•CH ₂ Br	175.1	174	168 ± 8 ^q
•CH ₂ BrH ⁺	1083.6	990	
CH ₃ CN	75.7	74 ± 1	
CH ₃ CNH ⁺	825.6	817	
•CH ₂ CN	267.2	245 ± 10	243 ± 12, ^s 250 ± 8 ^t
•CH ₂ CNH ⁺	1036.5	1004	
CH ₃ CHO	-174.3	-165.8 ± 0.4	
CH ₃ CHOH ⁺	589.3	583	
•CH ₂ CHO	16.6		
•CH ₂ CHOH ⁺	768.2		
CH ₃ NO ₂	-86.7	-74.8 ± 1	
CH ₃ NO ₂ H ⁺	700.4	705	
•CH ₂ NO ₂	125.9		
•CH ₂ NO ₂ H ⁺	905.3		

^a Values at 298 K in kJ mol⁻¹. ^b This value is different from the G2 value quoted by Armstrong et al.⁴⁷ due to an erroneous G2 total energy quoted in their paper. ^c Griller and Lossing.³⁴ ^d Ruscic and Berkowitz.³⁶ ^e Dóbe et al.⁴⁸ ^f Using $\Delta_f H^\circ_{298}(\text{CH}_2\text{OH}) = -16.6 \pm 0.9$ kJ mol⁻¹ (Ruscic and Berkowitz)³⁶ and PA(CH₂OH) = 695 ± 8 kJ mol⁻¹ (Audier et al.).⁴² ^g G2 value of -184.1 kJ mol⁻¹ for CH₃OCH₃ and +3.8 kJ mol⁻¹ for •CH₂OCH₃ using isodesmic reactions (Good and Francisco).⁴⁹ ^h Holmes and Lossing.⁵⁰ ⁱ Theoretical value of -240 ± 5 kJ mol⁻¹ by Espinosa-Garcia.⁵¹ ^j Using experimental PAs of the halomethanes (Glukhovtsev et al.).⁴⁴ ^k Pickard and Rogers.⁵² ^l J. L. Holmes (private communication as quoted by Gauld et al.).¹⁷ ^m Schweighofer et al.⁴⁵ ⁿ Ruscic and Berkowitz³⁷ corrected to 298 K. ^o Chou et al.⁴⁶ ^p Seetula.³⁸ ^q Holmes and Lossing.⁵³ ^r Ferguson et al.⁵⁴ ^s Holmes and Mayer.⁵⁵ ^t Matimba et al.⁵⁶

comparisons lying within the G2 target of ±10 kJ mol⁻¹ and only three differences (namely those for •CH₂BrH⁺, •CH₂CN, and •CH₂CNH⁺) being greater than 20 kJ mol⁻¹.

Concluding Remarks

Several important points emerge from this study.

(1) As is well established, hyperconjugative interactions in CH₃X molecules can take the form of (a) hyperconjugative

electron donation from an $n(X)$ orbital to a $\pi^*(CH_3)$ orbital in the case of π -donor substituents X or (b) hyperconjugative electron donation from a $\pi(CH_3)$ orbital to a $\pi^*(X)$ orbital in the case of π -acceptor substituents X.

(2) For π -donor substituents, protonation of CH_3X generally leads to a lengthening of the C–X bond due to an increase in the contribution of the no-bond resonance structure $^+CH_3 :XH$. This is accompanied by a sharp decrease in the heterolytic BDE of the C–X bond, to a value that is often lower than the corresponding homolytic BDE. Protonation also diminishes the hyperconjugative electron donation from $n(X)$ to $\pi^*(CH_3)$, thereby increasing the C–H bond strengths.

(3) For π -acceptor substituents, protonation of CH_3X enhances the hyperconjugative electron donation from $\pi(CH_3)$ to $\pi^*(X)$, thereby shortening the C–X bond relative to that in the unprotonated species. As with the π -donor substituents, protonation also serves to increase the contribution of the no-bond resonance structure $^+CH_3 :XH$, resulting in lower heterolytic BDEs.

(4) Conjugative interactions in $\cdot CH_2X$ radicals can take the form of (a) two-center three-electron interactions involving the $p(C)$ orbital and an $n(X)$ orbital in the case of π -donor substituents X or (b) three-center three-electron interactions involving the $p(C)$, $\pi(X)$, and $\pi^*(X)$ orbitals in the case of π -acceptor substituents X.

(5) For π -donor substituents, protonation of X in $\cdot CH_2X$ generally leads to a lengthening of the C–X bond due to an increase in the contribution of the no-bond resonance structure $^+CH_2 :XH$ as for the CH_3X molecules. This is again accompanied by a marked decrease in the heterolytic BDE of the C–X bond, to a value that is often lower than the corresponding homolytic BDE. Because protonation diminishes the degree of interaction between the $p(C)$ and $n(X)$ orbitals, the radical

stabilization energies (RSEs) calculated for the protonated radicals are negative, i.e., the $\cdot CH_2XH^+$ radicals are destabilized.

(6) For π -acceptor substituents, protonation of X in $\cdot CH_2X$ increases the conjugative interaction between $p(C)$ and the $\pi(X)$ system, resulting in a reduction in the C–X length relative to that in the unprotonated radicals. Because protonation increases the degree of interaction between the $p(C)$, $\pi(X)$, and $\pi^*(X)$ orbitals, the RSEs calculated for the protonated radicals are positive, i.e., the $\cdot CH_2XH^+$ radicals are stabilized.

(7) The proton affinities of $\cdot CH_2X$ radicals substituted by π -donor groups are found to be between 30 and 70 kJ mol^{-1} lower than those for their closed-shell counterparts. This can be understood in terms of a diminished availability of the lone-pair orbital resulting from interaction of $n(X)$ with the $p(C)$ orbital. For X = CHO and NO_2 , protonation occurs in a plane orthogonal to that of the $p(C)$ orbital and thus the PA is less influenced by the changes that occur in going from CH_3X to $\cdot CH_2X$.

Acknowledgment. We acknowledge the generous allocation of computer time on the Fujitsu VPP300 and SGI Power Challenge computers at the Australian National University Supercomputer Facility. M.N.G. gratefully acknowledges the award of a Visiting Fellowship at the Research School of Chemistry of the Australian National University.

Supporting Information Available: Total G2 energies and values of $\langle S^2 \rangle$ (Table S1) and GAUSSIAN archive entries for the MP2(full)/6-31G(d) optimized geometries (Table S2) (9 pages). See any current masthead page for ordering and Internet access instructions.

JA9728839